

Supporting Information

Amorphization of the Prototypical Zeolitic Imidazolate Framework ZIF-8 by Ball-milling

Shuai Cao,^a Thomas D. Bennett,^a David A. Keen,^{b,c} Andrew L. Goodwin,^d and Anthony K. Cheetham^{a*}

^a Department of Materials Science and Metallurgy, University of Cambridge, CB2 3QZ, UK

Tel: +441223767061; E-mail:akc30@cam.ac.uk

^b ISIS Facility, Rutherford Appleton Laboratory, Harwell Oxford, Didcot, OX11 0QX, UK

^c Department of Physics, University of Oxford, Clarendon Laboratory, Parks Road, Oxford, OX1 3PU, UK

^d Department of Chemistry, Inorganic Chemistry laboratory, University of Oxford, OX1 3QR, UK

SI-1: Synthesis routes of ZIF-8, ZIF-9 and ZIF-14

All the chemicals were used as purchased from their respective suppliers without any further purification. $\text{Zn}(\text{NO}_3)_2 \cdot 6\text{H}_2\text{O}$ (98%), 2-ethylimidazole (98%) and benzimidazole (98%) were procured from Sigma-Aldrich. ZnO (99.5%), $\text{Co}(\text{NO}_3)_2 \cdot 6\text{H}_2\text{O}$ (99%), imidazole (99+) and 2-methylimidazole (99%) were supplied by Acros Organics. The solvents used, namely methanol and N,N-dimethylformamide (DMF) (both lab reagent grade), were purchased from Fisher Scientific.

ZIF-8 in the nano form was synthesized according to the method devised by Cravillon.¹ ZIF-9 was produced by conventional solvothermal synthesis.² ZIF-14 was mechanochemically synthesized.³

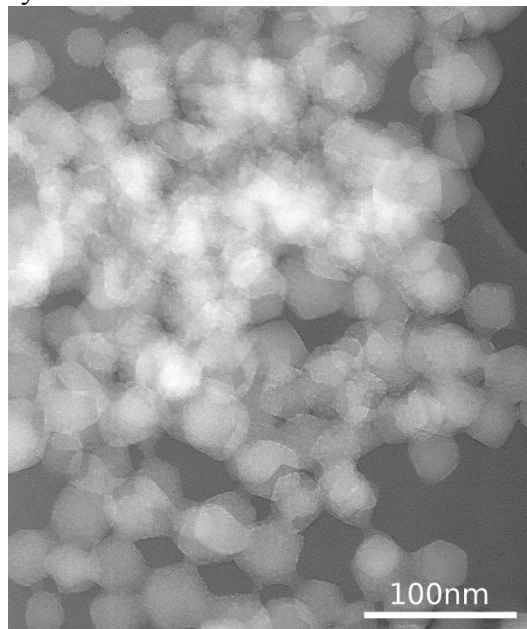


Figure S1: Bright filed TEM image of ZIF-8

SI-2: Ball-milling Amorphization

In all cases, around 150 mg of the relevant ZIFs were placed inside a 10 mL stainless steel jar alongside a 10 mm stainless steel milling ball at room temperature and sealed properly. This combination was then subjected to 30 Hz milling in a Retsch MM400 grinder mill for varying times. After milling, the amorphous milling products were recovered and characterized.

SI-3: Powder X-ray Diffraction (PXRD) measurements

Room temperature PXRD data of ZIF-8 and ZIF-14 (2θ range 5-60°) were collected with a Bruker-AXS D8 diffractometer using $\text{Cu K}\alpha_1$ ($\lambda = 1.540598 \text{ \AA}$) radiation and a LynxEye position sensitive detector in Bragg-Brentano parafocusing geometry. Analysis of the data was carried out using the X'pert HighScore Plus program. PXRD data of ZIF-9 were collected on a Philips PW1820 diffractometer using $\text{Cu K}\alpha_1$ radiation fitted with a graphite secondary monochromator.

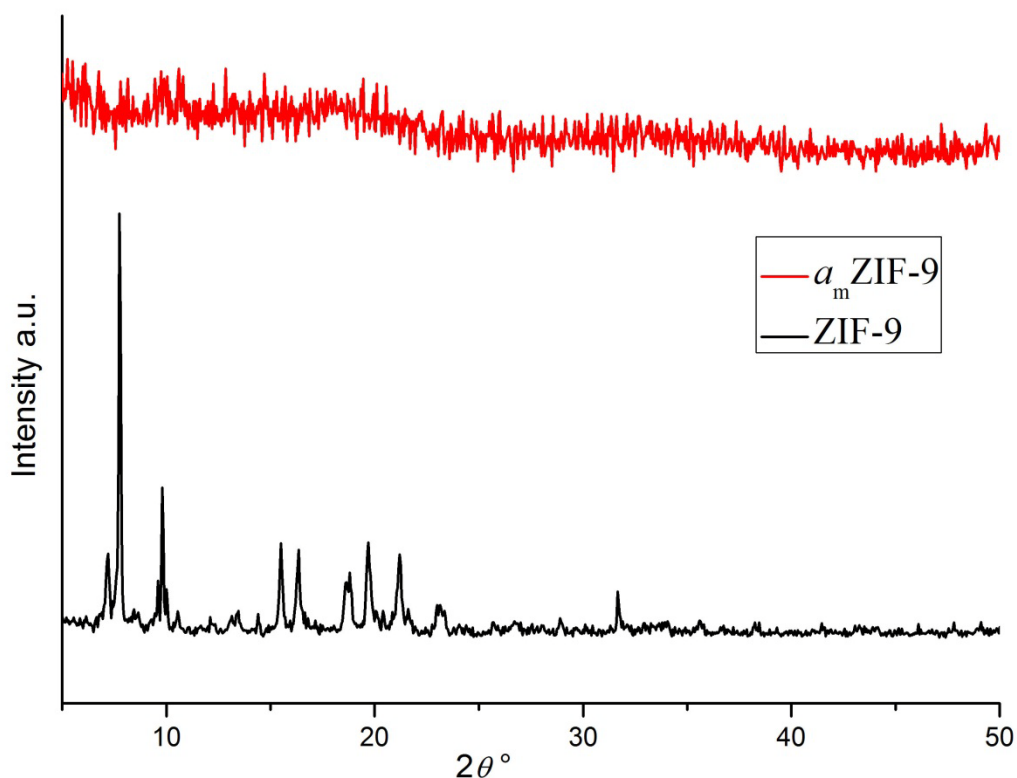


Figure S2: PXRD of ZIF-9 and a_m ZIF-9.

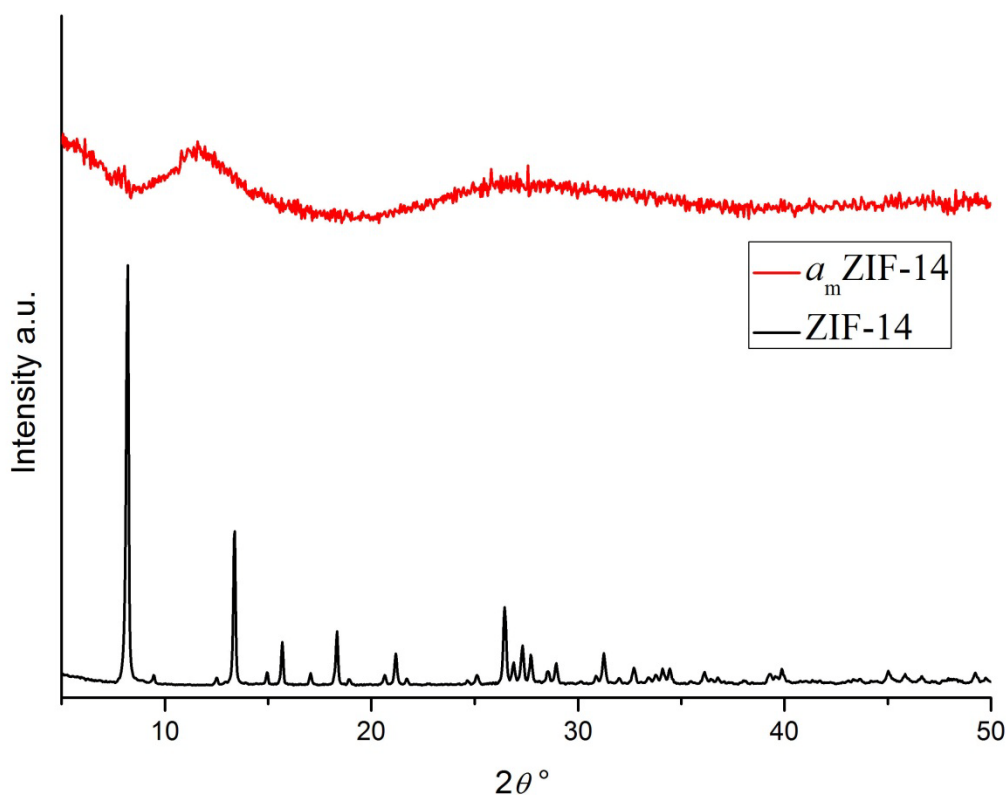


Figure S3: PXRD of ZIF-14 and a_m ZIF-14.

SI-4: Helium Pycnometry

Density values of both crystalline and amorphous samples were collected using a Micromeritics Accupyc 1340 helium pycnometer, equipped with a 1 cm³ insert. Typically, sample masses of between 100 and 150 mg were used and the values quoted are the mean and standard deviation from a cycle of 15 measurements. Before density measurements, all samples were degassed thoroughly under vacuum (< 1 mbar) at 150 °C for 5 hours.

Table S1: Helium pycnometry densities of ZIF-4, -8, -9 and -14 in both crystalline and 30 min milling-amorphized forms. (Unit: g cm⁻³)

	ZIF-4 ⁴	ZIF-8	ZIF-9	ZIF-14
Crystalline	1.4616(5)	1.450(1)	1.8496(8)	1.404(6)
Amorphous	1.576(4)	1.500(1)	1.861(2)	1.444(1)

Table S2: Atomic number densities of the α_m ZIF-4, -8, -9 and -14 based on the above helium pycnometry densities. (Units: atoms Å⁻³)

ZIF-4 ⁴	ZIF-8	ZIF-9	ZIF-14
0.0806(4)	0.0913(1)	0.1108(2)	0.0986(1)

SI-5: N₂ Sorption Porosimetry

Porosity was measured by N₂ sorption isotherm at 77 K on a Micromeritics ASAP 2020 instrument. Samples were outgassed in vacuum (~5 µbar) for at least 5 hours at 423 K before starting the sorption measurements. The surface areas were estimated using the Brunauer–Emmett–Teller (BET) equation for the relative pressure range (P/P₀) of 0.002 to 0.3. The saturation pressure, P₀, corresponds to ca. 103.4 kPa. The t_{HJ}-plot micropore volume is the calculated total pore volume with dimensions < 20 Å, using the Harkins and Jura method.

SI-6: Thermal Gravimetric Analysis (TGA)

Thermal gravimetric analysis was performed on TA Instrument Q600 (simultaneous TGA-DSC). Typically, 10 mg of sample was placed in an alumina pan under dry N₂ flow (100 mL/min) and heated at a rate of 10 °C/min to 1000 °C. Before TGA measurements, all samples were degassed thoroughly under vacuum (< 1 mbar) at 150 °C for 5 hours.

Table S3: Decomposition temperatures of α_m ZIF-8 milled for different times.

Milling Time/min	0	10	20	30	300
Decomposition Temperature/°C	486	464	453	418	350

Note: Decomposition temperature was defined as the temperature when sample loses 5% of its initial weight.

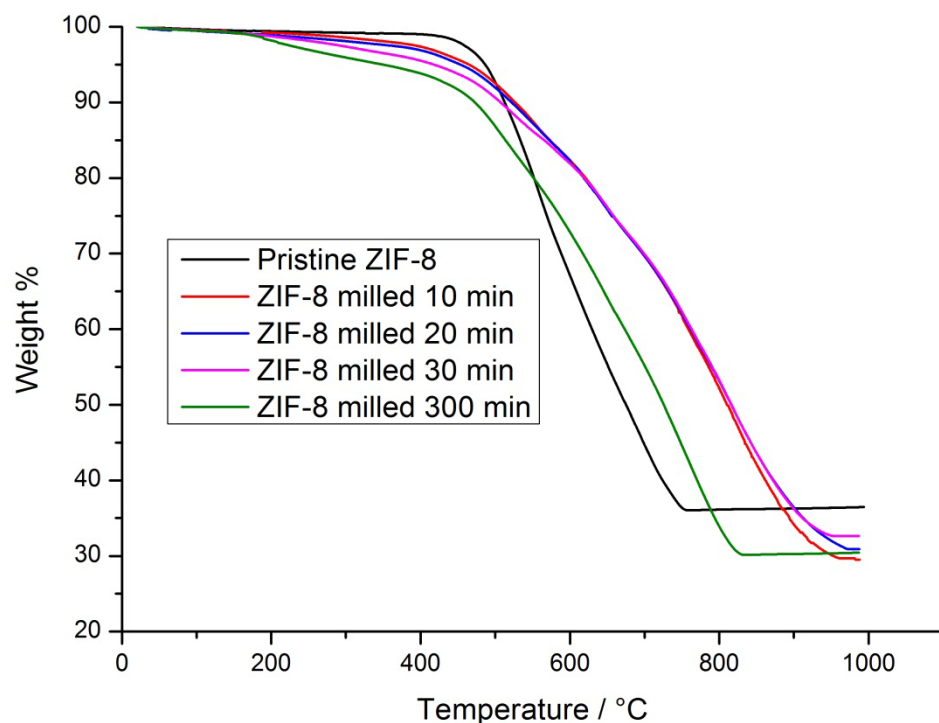


Figure S4: TGA of ZIF-8 ball-milled for different times under N₂ purge flow.

The lower weight retention of the amorphous materials is probably due to some ZnO residual being reduced to elemental Zn, which is lost above 800 °C.⁵

SI-7: X-ray total scattering and Pair Distribution Function (PDF)

The equipment used is a Ag-source X'pert Pro MPD lab diffractometer ($\lambda = 0.561 \text{ \AA}$). Data collection was performed using loaded 1.0 mm diameter silica capillaries and collection times of approximately 40 hrs. Data were corrected for experimental effects using the GudrunX⁶ program to produce total scattering structure factors, $S(Q)$, and pair distribution functions, $G(r)$ (the sine Fourier transform of $S(Q)$).

Table S4: Structural correlation distances in a_m ZIFs. (M...M refers to Zn...Zn for a_m ZIF-4, -8 and -14; in the case of a_m ZIF-9, it refers to Co...Co.) (Unit: Å)

	M...M Peak in $G(r)$	Average M...M distance in crystalline structure*	Approximate broad hump peak position in $G(r)$
ZIF-4 [Zn(Im) ₂]	5.94	5.90	12.6
ZIF-8 [Zn(mIm) ₂]	6.04	6.01	14.2
ZIF-9 [Co(bIm) ₂]	5.80	6.00	N/A
ZIF-14 [Zn(eIm) ₂]	6.12	6.07	17.1

*Values obtained from crystalline structure cif. files.

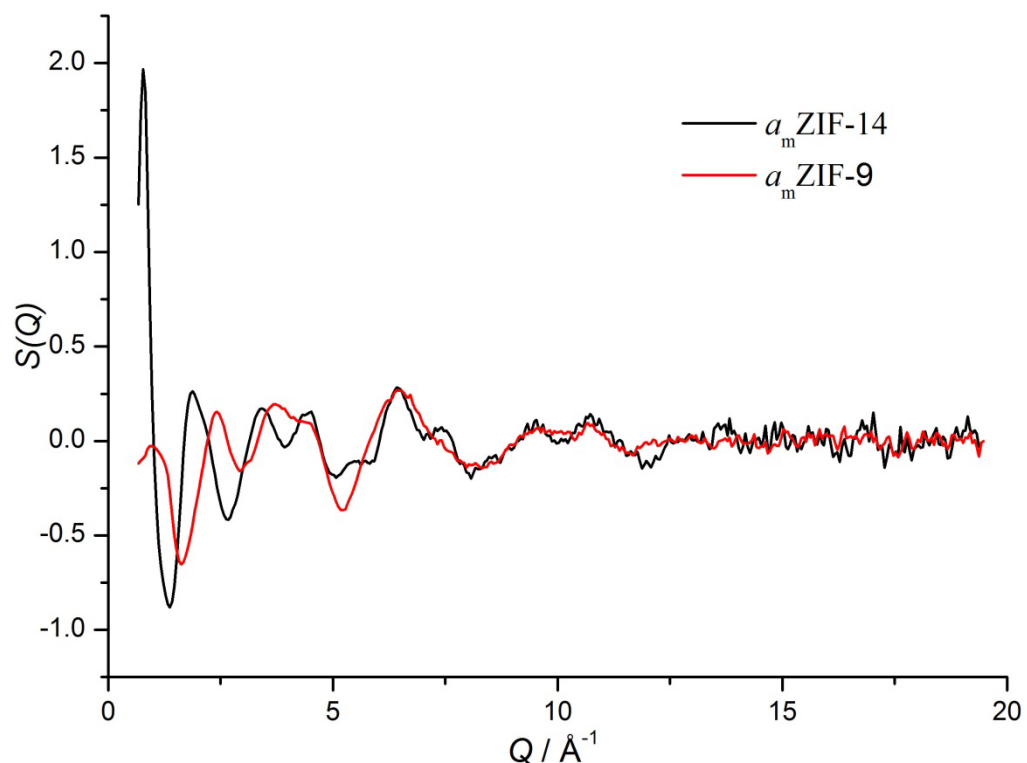


Figure S5: X-ray total scattering data on a_m ZIF-9 and -14.

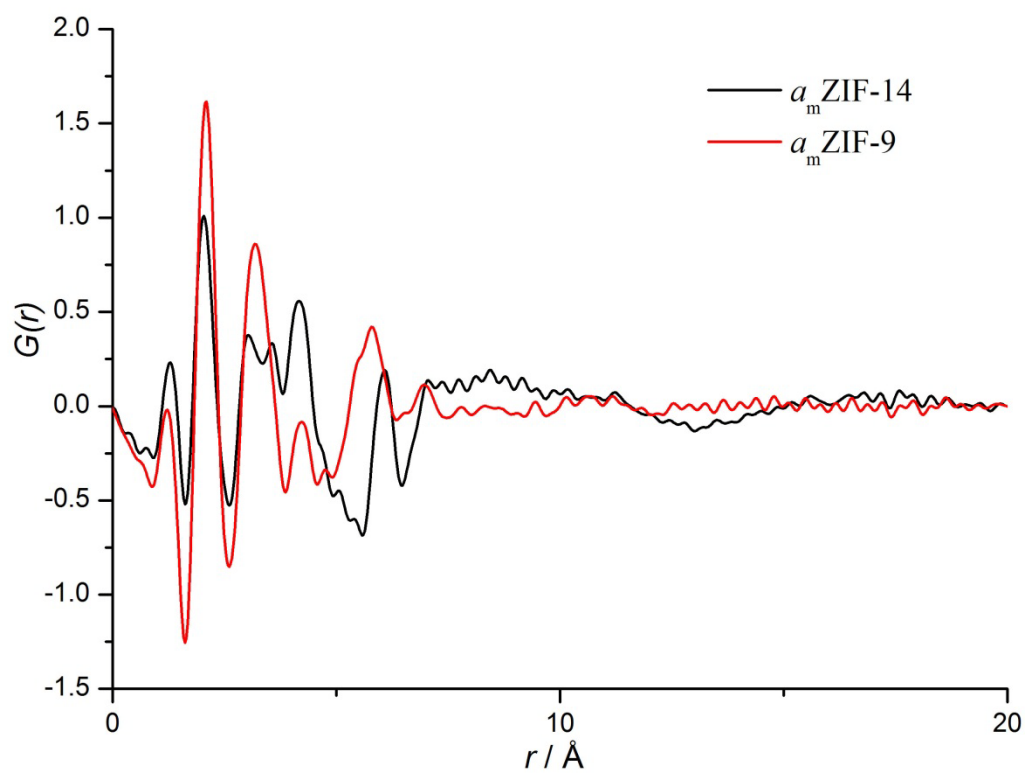


Figure S6: PDFs data on a_m ZIF-9 and -14.

SI-8: Reverse Monte Carlo (RMC) modelling

The RMC modelling was carried out using the program RMCProfile⁷. A configuration of a_m ZIF-8 was generated based on the previous model of unsubstituted a_m ZIF-4⁸ adjusted to the measured a_m ZIF-8 density and with the addition of a 2-methyl group on each imidazolate ion. The model therefore consisted of 512 [Zn(mIm)₂] formula units in a 50.303 Å length cubic box. The topology of the continuous random network structure was retained through the use of ‘distance window’ restraints and implicit in the way that the program minimised the molecular geometry. Initially the model was minimised via a potential-only refinement (i.e. data-free) to relax the initial structure. Following this the X-ray $S(Q)$ data were also incorporated in the RMCProfile ‘cost function’ and the model was refined until convergence.

SI-9: Transmission Electron Microscopy (TEM)

Nano form ZIF-8 samples for TEM were prepared by pipette dropping of a very small amount of the fresh ZIF-8 suspensions onto holey carbon films supported on standard Cu 300 mesh TEM grids. Then the methanol solvent was allowed to evaporate. Bright field images were collected using a JEOL 2000FX TEM operating at 200 keV, maintaining the electron dose as low as possible, consistent with obtaining acceptably sharp images.

SI-10: Fourier Transform Infrared Spectroscopy (FT-IR)

FT-IR analysis was carried out using the Bruker Tensor 27 Infrared Spectrometer, which is fitted with an attenuated total reflectance (ATR) cell to allow fast data collection. The data was collected in the wavenumber range of $520 - 4000\text{ cm}^{-1}$ at a resolution of 4 cm^{-1} .

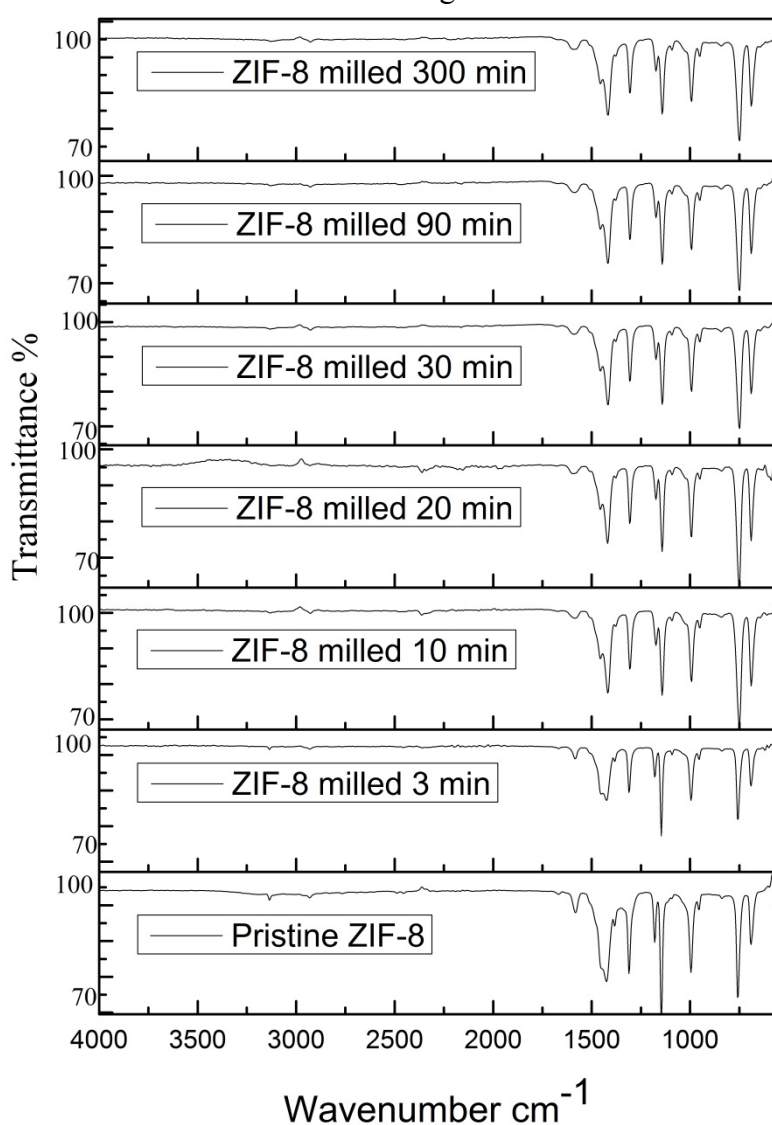


Fig. S7: FT-IR data of ZIF-8 milled for various times. There are no substantial changes of the IR spectra due to milling.

SI-11:Elemental Analysis

Elemental analysis was carried out at the Department of Chemistry, the University of Cambridge (UK) as a technical service.

Table S5: CHN elemental analysis results of ZIF-8 milled for various times.

Milling time / minutes	C content / wt %	H content / wt %	N content / wt %
Calculated	42.22	4.40	24.63
0	41.73	4.40	24.02
3	41.49	4.34	24.03
10	41.33	4.31	23.80
20	41.14	4.33	23.88
30	41.38	4.33	23.72
90	41.05	4.29	23.58
300	40.75	4.26	23.76

There are no substantial changes of chemical composition from the starting material due to ball-milling.

References

1. J. Cravillon, S. Münzer, S.-J. Lohmeier, A. Feldhoff, K. Huber and M. Wiebcke, *Chemistry of Materials*, 2009, **21**, 1410-1412.
2. K. S. Park, Z. Ni, A. P. Cote, J. Y. Choi, R. Huang, F. J. Uribe-Romo, H. K. Chae, M. O'Keeffe and O. M. Yaghi, *Proc Natl Acad Sci U S A*, 2006, **103**, 10186-10191.
3. P. J. Beldon, L. Fábián, R. S. Stein, A. Thirumurugan, A. K. Cheetham and T. Friščić, *Angewandte Chemie International Edition*, 2010, **49**, 9640-9643.
4. T. D. Bennett, S. Cao, J. C. Tan, D. A. Keen, E. G. Bithell, P. J. Beldon, T. Friscic and A. K. Cheetham, *Journal of the American Chemical Society*, 2011, **133**, 14546-14549.
5. S. J. Yang, T. Kim, J. H. Im, Y. S. Kim, K. Lee, H. Jung and C. R. Park, *Chemistry of Materials*, 2012, **24**, 464-470.
6. A. K. Soper and E. R. Barney, *Journal of Applied Crystallography*, 2011, **44**, 714-726.
7. M. G. Tucker, D. A. Keen, M. T. Dove, A. L. Goodwin and Q. Hui, *Journal of Physics: Condensed Matter*, 2007, **19**, 335218.
8. T. D. Bennett, A. L. Goodwin, M. T. Dove, D. A. Keen, M. G. Tucker, E. R. Barney, A. K. Soper, E. G. Bithell, J. C. Tan and A. K. Cheetham, *Physical Review Letters*, 2010, **104**, 115503.